THE JOURNAL OF COMPARATIVE NEUROLOGY 298:50–68 (1990)

Visual Projections Induced Into the Auditory Pathway of Ferrets. I. Novel Inputs to Primary Auditory Cortex (AI) From the LP/Pulvinar Complex and the Topography of the MGN-AI Projection

SARAH L. PALLAS, ANNA W. ROE, AND MRIGANKA SUR
Department of Brain and Cognitive Sciences, Massachusetts Institute of Technology, Cambridge, Massachusetts 02139

ABSTRACT

The organization of cortical circuitry responsible for processing sensory information is a subject of intense examination. However, it is not known whether cortical cells in different sensory cortices process information in a way that is specific to the modality of their input, or whether there are commonalities in processing circuitry across different cortices. In our laboratory, this question has been investigated at the level of the geniculocortical pathway by routing information of one sensory modality into the processing circuitry of another modality. Appropriate early lesions cause growth of retinal axons into the auditory thalamus (MGN) (Sur et al., Science *242:*1437, '88). Previously, we have established that the MGN carries the resulting visual information on to primary auditory cortex (AI), which thus contains visually responsive neurons and a topographic representation of the retina (Roe et al., Soc. Neurosci. Abstr. *14:*460, '88; Sur et al., Science *242:*1437, '88). In this paper, we describe anomalous projections from the dorsal part of the thalamus, specifically the lateral posterior/pulvinar complex, into AI. This result demonstrates that thalamic neurons belonging to one modality can be induced to project to cortex that is normally of a different modality. In addition, we have studied in detail the nature of the MGN to AI projection in these animals as compared to the normal projection. The MGN to AI projection appears to be unaltered by the lesions; the location and topography of labelled cells are similar to that in normal animals. Because the MGN to AI projection is still highly divergent along the "isofrequency" dimension when compared to the tonotopic dimension, our data suggest that visual topography in the cortical map is created within the auditory cortex, perhaps by activity-dependent sharpening of the retinal representation during development.

Key words: cross-modal plasticity, neocortical development, sensory neocortex, topographic maps, afferent/target matching

In passing from the thalamus to the cortex, sensory information is transformed with respect to the topographic mapping of the sensory epithelium and the receptive field properties of individual cells. These transformations could occur in several ways. First, specific inputs from the thalamus might induce specific patterns of circuitry in their target sensory cortex during development. Second, a sensory cortical area might develop its unique processing circuits independent of input from the thalamus. It is also possible that certain aspects of information processing might be common across different sensory neocortices, regardless of the modality of the input.

To address these issues, we have employed a mammalian system in which afferents of one modality are rerouted early in development to regions of thalamus and cortex that normally process information of a different modality. In the ferret, ablation of central retinal targets and deafferentation of the auditory thalamus allow the retina to terminate in the auditory thalamus (Sur et al., '88). This phenomenon has also been described in hamsters by Schneider ('73) and

Accepted April 11, 1990.

Address reprint requests to Sarah L. Pallas, Dept. of Brain & Cognitive Science, E25-618, M.I.T., Cambridge, MA 02139.

Frost ('81, '86). In previous studies, we have demonstrated that in lesioned animals, the auditory thalamus (specifically, the medial geniculate nucleus, or MGN) transmits visual rather than auditory information to primary auditory cortex (AI) (Sur et al., '88). As a result, single cells in AI respond to visual stimulation. We have also demonstrated that a retinotopic map is established in AI as a result of its novel visual inputs (Roe et al., '88; Sur et al., 90). These ferrets with rerouted retinal projections provide a unique opportunity for studying the degree and extent to which inputs determine the intrinsic and extrinsic connectivity patterns of target structures during development.

The purpose of the present investigation is two-fold. First, we wish to determine whether the MGN is the sole source of visual input to AI in lesioned animals, or whether other visual structures might contribute to the visual response properties of AI. The present paper will deal with thalamic inputs, and a subsequent paper with cortical inputs (Pallas et al., in prep.). Additional sources of visual input to AI could be derived from stabilization of early exuberant projections, or from sprouting of novel connections. We have also briefly addressed changes in outputs of AI as a result of the early lesions.

Our second goal is to compare, in overall pattern and internal detail, the connections between MGN and AI in lesioned and normal ferrets. Such a comparison directly addresses whether or not the nature of the peripheral input regulates thalamocortical connectivity.

We have employed tracer injections in AI of adult ferrets that received neonatal lesions redirecting retinal axons into the MGN and have compared the pattern of thalamic projections to AI in these lesioned animals with those in normal ferrets. Our results indicate that the type of input to the auditory thalamus plays relatively little direct role in establishing the connections characteristic of the auditory thalamocortical pathway. A preliminary report of our results has appeared previously (Pallas et al., '88).

Abbreviations

aes	anterior ectosylvian sulcus
AI	primary auditory cortex
CP	cerebral peduncle
dLGN	dorsal division of the lateral geniculate nucleus
FB	Fast Blue
FG	Fluoro-Gold
GW	geniculate wing, or retinal recipient zone of the pulvinar
HRP	horseradish peroxidase
LG	lateral gyrus
LM-Sg	lateromedial-suprageniculate area of the thalamus
LP	lateral posterior nucleus
LS	lateral suprasylvian cortex
MGN	medial geniculate nucleus
MGv	ventral division of the MGN
MGm	medial division of the MGN
MGd	dorsal division of the MGN
pes	posterior ectosylvian sulcus
PO	posterior thalamic group
pss	pseudosylvian sulcus
PT	pretectum
Pul	pulvinar
R	Rhodamine
SC	superior colliculus
SGS	stratum griseum superficiale of the superior colliculus
SSG	suprasylvian gyrus
VB	ventrobasal nucleus of the thalamus
WGA-HRP	wheat germ-agglutinated horseradish peroxidase

METHODS

Animals

A total of six normal and five experimental (lesioned) ferrets were used in this study (Table 1). All were pigmented ferrets (*Mustela putorius furo,* Family Mustelidae, Order Carnivora) obtained from Marshall Farms (North Rose, NY). Neonatal ferrets were from dams that were bred at Marshall Farms and shipped to us prior to delivery. Gestation time in ferrets is 42 days. The colony was maintained on cat food and water with a 14:10 light:dark cycle.

Neonatal surgery

All neonatal surgeries for these experiments were done on the day of birth. Each kit was anesthetized by deep hypothermia. The skull was exposed by an incision in the overlying skin, after which the posterior portion of the brain was visualized by removal of part of the skull with a scalpel. Under microscopic observation, the superior colliculus and the back of the cortex corresponding to cortical areas 17 and 18 were unilaterally cauterized in order to remove the major targets of the retina (the dLGN atrophies severely as a result of the cortical lesion.). At the same time, the MGN was deafferented by sectioning the brachium of the inferior colliculus. The skin was then sutured, an injection of antibiotic (Amoxicillin, 1 mg) was given, and the kit was revived under a heat lamp. Kits were returned to their dams until weaning at 8 weeks and were then reared to adulthood (15 weeks or more).

Tracer injection

Adult ferrets used for injection of tracers were anesthetized with ketamine (30–40 mg/kg) and xylazine (1–3 mg/kg). Atropine (0.04 mg/kg) and dexamethasone (0.7 mg/kg) were given at the same time to prevent congestion and reduce swelling, respectively. Heart and respiration rate were monitored closely throughout the surgery and supplemental half-doses of ketamine were given as needed. Body temperature was maintained at 38°C. The skull was stabilized in a stereotaxic apparatus, and the cranium and dura overlying the auditory cortex were removed. All pressure points were infiltrated with lidocaine. Neuroanatomical tracers were then injected into AI with a 1 μl Hamilton syringe. All injections were located in the medial ectosylvian gyrus, the location of the primary auditory cortex in the ferret (Kelly et al., '86; Phillips et al., '88). Amounts and concentrations of tracers that we used were as follows: HRP/WGA-HRP (20%/2% in distilled water, 50–100 nl), Rhodamine-labelled beads (25% in distilled water, 500 nl), Fluoro-Gold (4% in distilled water, 50–100 nl), and Fast Blue (5% in distilled water, 50–100 nl). Injections of multiple tracers allowed us to topographically map the projections to and from AI. Locations of the injections were noted on a drawing of the cortical surface. After survival times of 5–7 days, the animal was overdosed with sodium pentobarbital and perfused with a 1% paraformaldehyde, 2% glutaraldehyde fixative for HRP histochemistry, or a 4% paraformaldehyde fixative if fluorescent tracers were used. Frozen sections were cut at 50 μm in the coronal plane. Horseradish peroxidase (HRP) was developed using tetramethylbenzidine (TMB) as the chromogen (Mesulam, '78). Fluorescent-labelled sections were quickly dehydrated, cleared, and coverslipped with a non-fluorescent

mounting medium (Krystalon). Nissl and, in some cases, acetylcholinesterase stains (Geneser-Jensen and Blackstad, '71; Karnovsky and Roots, '64) on alternate sections were used to define brain areas in which label was found.

Electrophysiological mapping

In some of the animals that received brain injections, a visual field map was made by recording extracellularly in AI prior to perfusion. This provided confirmation of the boundaries of visually responsive primary auditory cortex and confirmed that our injections were within these boundaries. The procedure for physiological mapping in the ferret brain has been described elsewhere (Sur et al., '88). Briefly, single or multiunit activity was recorded with parylene-insulated tungsten microelectrodes while searching the visual field with bars and spots of light. A pair of stimulating electrodes located in the optic chiasm was used to electrically stimulate retinal axons. The cortical surface was mapped with respect to receptive field location of visual activity. The results of the mapping experiments have been reported elsewhere (Roe et al., '88; Sur et al., '90).

Eye injections

To determine whether cells projecting from thalamus to AI overlap with retinal terminal arbors in the thalamus, injections of HRP were made in one eye in each of two normal and three lesioned ferrets. Following anesthesia with ketamine/xylazine as described above, 20 μl of a solution of 20% HRP/4% WGA-HRP in distilled water were injected in the posterior chamber of the eye with a Hamilton syringe. An opthalmic antibiotic mixture (bacitracin/neomycin/polymixin) was applied to the eye and a subcutaneous injection of Amoxicillin (100 mg/ml, 0.1 cc) was given to prevent infection. After a survival time of 4 days, the animal was overdosed with sodium pentobarbital and perfused with a 1% paraformaldehyde 2% glutaraldehyde fixative, the brain was sectioned frozen at 50 μm in the coronal plane, and alternate sections were reacted with TMB or for Nissl substance as described above.

TABLE 1. Animals Receiving Tracer Injections in AI

Animal	Figure	Lesion	Tracer	Transport
F88-1		No	HRP	Good
F88-5		No	HRP	Good
F88-33		No	HRP	Poor
			R	Good
			FG	Good
F88-39	5	No	HRP	Good
			R	Poor
			FB	Good
F88-53	1, 6	No	HRP	Good
F89-90	4	No	HRP	Good
F88-16		Yes	HRP	Poor
F88-24		Yes	HRP	Good
			R	Poor
			FG	Good
			FB	Poor
F88-34	10	Yes	HRP	Good
			R	Good
			FG	Good, LS/AI injection
F88-61	7, 9	Yes	HRP	Good
			R	Good
			FG	Good
			FB	Good
F88-76	8	Yes	HRP	Poor
			R	Poor
			FG	Good
			FB	Good

RESULTS

Quality of injections and transport

In all cases except those specifically mentioned, the injection site and the halo of label surrounding it were within the boundaries of the anterior and posterior ectosylvian and the middle suprasylvian sulci, which in the ferret delineate AI (Kelly et al., '86; Phillips et al., '88). The extent of diffusion of label around the injection site varied with the tracer used. Diffusion was greatest with HRP (0.6–1.6 mm diameter). A large HRP injection site in AI is pictured in Figure 1. Rhodamine injections produced the most circumscribed injection site (0.4–0.6 mm). Fast Blue and Fluoro-Gold injection halos varied from 0.4–1.4 and 0.6–0.8 mm, respectively. It was important to prevent the injection syringe from extending into the white matter. When this occurred, the pattern of retrogradely transported label was more extensive, labelling structures that did not contain label following more shallow injections. These cases were eliminated from the data presented here.

All four of the tracers we used gave good retrograde label in both thalamus and cortex. In our hands, Fluoro-Gold was perhaps the most reliable of the tracers. In addition, both Fluoro-Gold and HRP/WGA-HRP-labelled terminal arbors and boutons anterogradely from cortical injections. The WGA-HRP terminal label was of a diffuse punctate quality, with occasional fine fibers labelled. The anterograde label with Fluoro-Gold was more dense, in some cases filling large portions of terminal arbors very clearly. In general, the quality of anterograde label was much better in the thalamus than in the cortex.

Confirmation of lesions in neonatally lesioned animals

Confirmation that the lesions were of sufficient magnitude was made qualitatively from inspection of the cortical surface and from Nissl-stained coronal sections (Fig. 2). The lesions themselves were fairly reproducible between animals. In some cases, damage to the superior colliculus extended somewhat bilaterally. The cortical lesions invariably removed the majority of Area 17 and usually most of Area 18. In some cases there was also some damage rostral to Area 18. The dLGN was never completely degenerated, but in all cases was much smaller than normal. It is unclear whether the incomplete degeneration of dLGN, particularly of the A layers, results from incomplete lesions of areas 17 and 18, or whether some cells in dLGN are not dependent on those cortical areas for their survival. A complete removal of Areas 17 and 18 is difficult because these areas extend far laterally along the lateral convexity of each hemisphere as well as medially down the medial wall.

Identification of brain structures

Because there is no brain atlas currently available for the ferret, our identifications of thalamic nuclei are made from Nissl-stained sections by comparing locations and cytoarchitecture of nuclei with those in cats (Berman and Jones, '82). The gross structure of the ferret thalamus is quite similar to that of the cat, although some differences do exist. Among the visual thalamic nuclei, the dLGN and LP/Pulvinar complex are rotated ventrolaterally in the ferret relative to their position in the cat. We have limited our identification of extrageniculate thalamic regions to distinguish between LP and the pulvinar only, and we have not attempted to subdivide the LP nucleus into distinct regions.

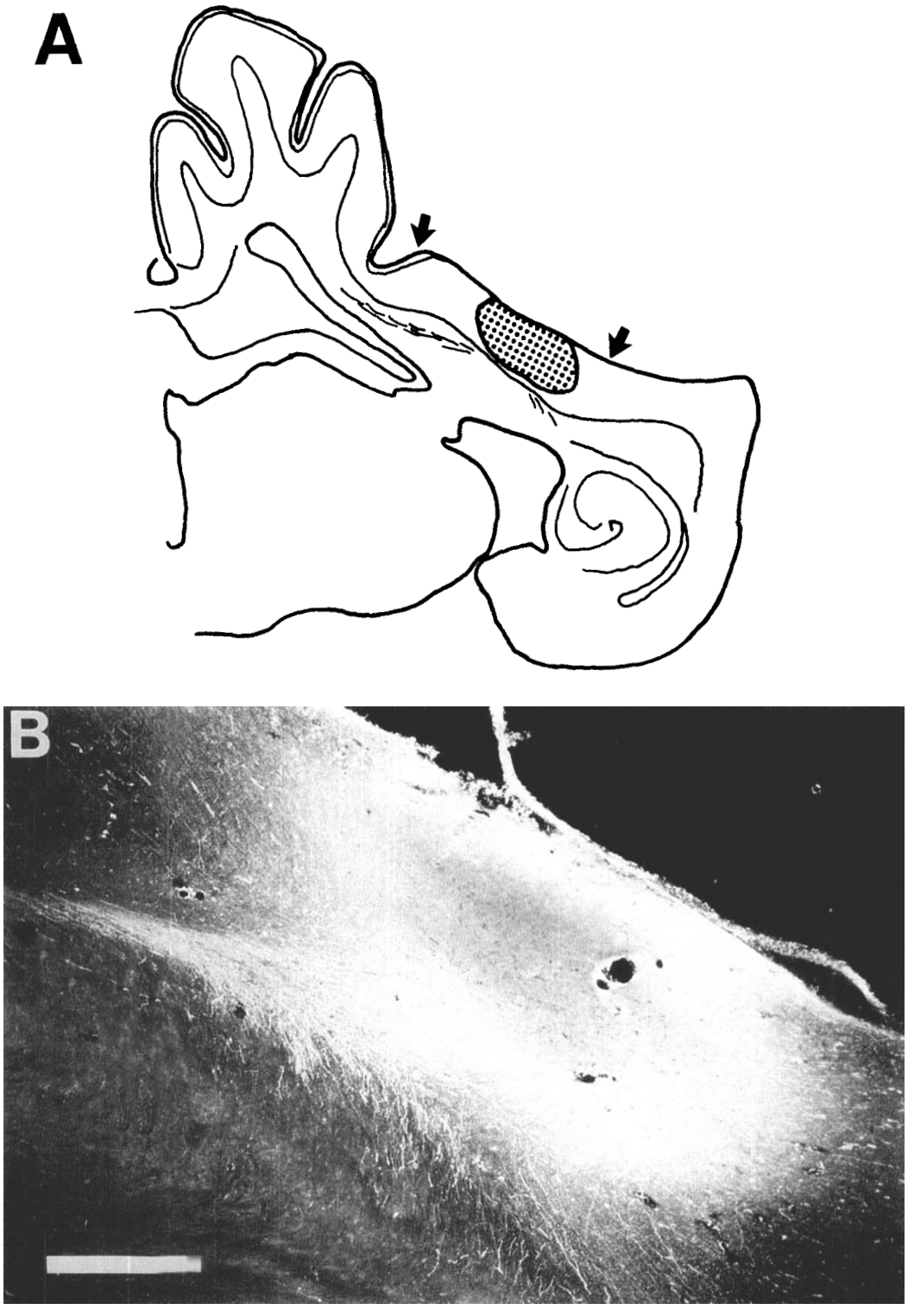

Fig. 1. An HRP injection site in AI. This figure shows the site where an injection of HRP mixed with WGA-HRP was made into the primary auditory cortex (AI). The tissue was reacted for HRP using tetramethylbenzidine (TMB)' as the chromagen. **A:** In this low-power view, the placement of the injection site in AI between the anterior ectosylvian sulcus and the pseudosylvian sulcus can be seen. The two arrows delineate the dorsal and ventral borders of AI as determined by cytoarchitectonic criteria in the adjacent Nissl-stained section. **B:** This higher-power micrograph is from an adjacent section counterstained with Neutral Red. A small hole can be seen where the Hamilton syringe penetrated the tissue. Most of the fibers leading away from the injection site are headed for the internal capsule and the cerebral commissure, and a few terminate or originate in the ipsilateral cortex. Scale bar: 0.5 mm.

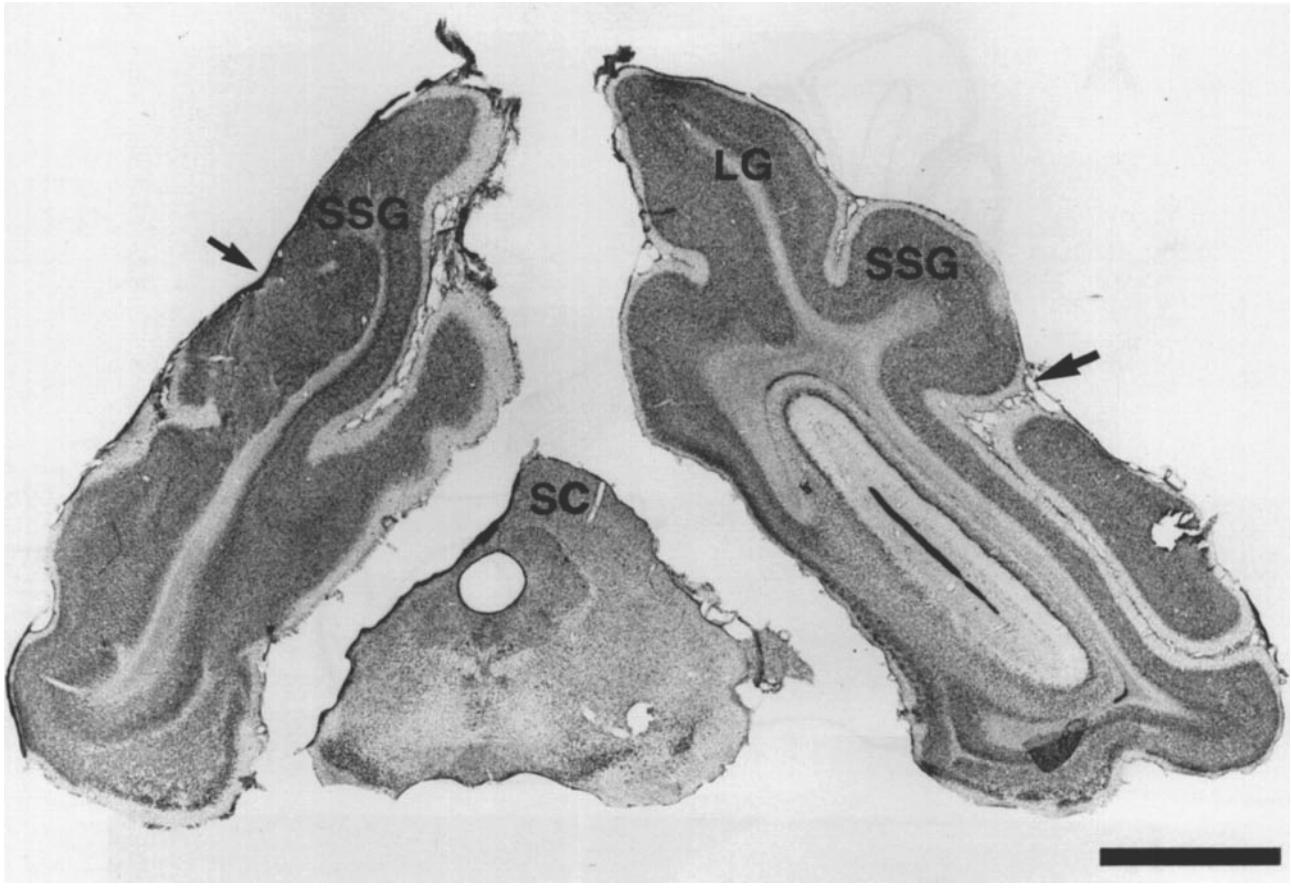

Fig. 2. A coronal section through the brain of an adult ferret which received unilateral lesions of the visual cortex and superior colliculus, and section of the brachium of the inferior colliculus as a neonate. The superior colliculus is completely absent, as can be seen clearly here. Also, as seen from the abnormal sulcal pattern, most of the lateral gyrus (LG) containing visual cortical areas 17 and 18 is missing. The arrows on each side point to the suprasylvian sulcus. The dLGN is shrunken markedly as a result (not shown, but see Figs. 7 and 12). The hole in the right ectosylvian gyrus is the result of an injection syringe. Scale bar: 3 mm.

This would require more connectional data than is presently available for the ferret. The pulvinar can be easily identified in Nissl-stained sections by the heavy fiber bundles running through it. Similarly, among the auditory thalamic nuclei, we do not distinguish the subnuclei of the MGN beyond identifying the ventral, dorsal, and medial components. We have drawn the borders of these MGN subdivisions only in those sections in which they were clear. In the case of the MGN, the size, shape, and orientation of cell somata aid in identification (Morest, '64, '65). Cortical area AI was identified by its location within the anterior and posterior limbs of the ectosylvian sulci (Phillips et al., '88) and by cytoarchitectonic criteria. The extent of AI was defined in individual sections by its cytoarchitectonic characteristics, chiefly the density and thickness of layers IV and V (Fig. 3) (Rose, '49; Sanides and Hoffmann, '69; Otsuka and Hässler, '62).

Thalamocortical projections in normal animals

The pattern of thalamic label after injections into AI in normal ferrets is illustrated in Figure 4. As expected, the majority of the retrograde label following AI injections in normal animals was found in the MGN. The ventral, dorsal, and medial divisions of MGN all contained label, with the heaviest label in the ventral and medial divisions. The label in the ventral division was quite heavy in the anterior half of its rostrocaudal extent and lightest in the caudal portion. In addition, heavy retrograde label was seen in the posterior thalamic group (PO). The caudal region of the dorsal division was devoid of label. Figure 5 shows a reconstruction of the pattern of retrograde thalamic label in a normal ferret resulting from injections of Fast Blue and HRP in two separate locations in AI. Each symbol in the figure represents two to three individual labelled cells. Anterograde label is not shown in this or any of the other reconstructions. As can be seen in the figure, the thalamic input to AI arises from several cell groups and from extensive slabs of cells in the ventral division of the MGN. This is similar to what has been described in the cat; that is, the MGN-AI projection is highly divergent and convergent (Merzenich et al., '82, '84; see, however, Brandner and Redies, '90). Furthermore, Figure 5 shows that injections at two different sites in AI can, depending on their location, produce label in two separate slabs in the ventral division of MGN, showing the segregation between what are probably different frequency representations in this nucleus (Andersen et al., '80, Merzenich et al., '82).

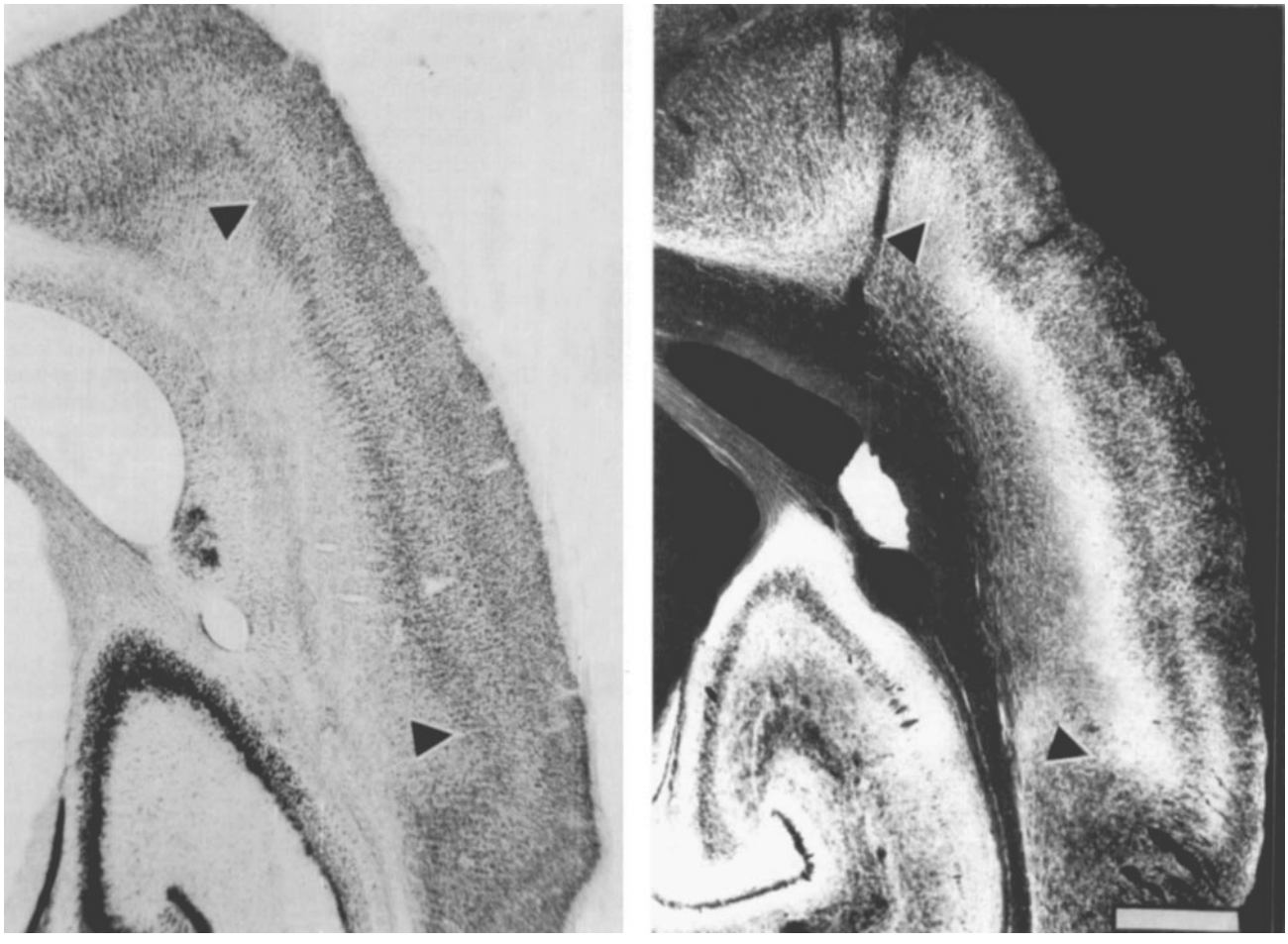

Fig. 3. Cytoarchitectonic determination of the borders of AI. The arrowheads show the upper and lower boundaries of AI. The figure on the left is a Nissl stain in which several characteristics of AI can be seen: the cell-sparse layer V, the absence of large pyramidal cells in layer V, and the large, densely packed layer IV. The figure on the right is the adjacent section (100 μm anterior) stained for acetylcholinesterase and photographically reversed for better contrast. The acetylcholinesterase staining highlights AI. Note the dense staining in layers IV and VI. The anterior and posterior borders of AI are defined by the anterior and posterior ectosylvian sulci (Kelly et al., '86; Phillips et al., '88). Scale bar: 1 mm.

Another reconstruction of retrograde thalamic label following an HRP injection in AI of a normal ferret is shown in Figure 6. As in Figures 4 and 5, label is restricted to the three main divisions of the MGN and to PO. The thalamic label extends quite far in the rostrocaudal direction. There is no label in the most caudal portion of MGN, as seen in the other animals.

Corticothalamic projections in normal animals

The pattern of anterograde label in the thalamus following injections in AI was quite similar to the pattern of retrograde label. Terminals were found most heavily in the ventral division of AI but were also present in the medial and dorsal divisions and in PO. This strict reciprocation of thalamocortical and corticothalamic projections is also seen in the auditory system of the cat (Andersen et al., '80).

Thalamocortical projections in lesioned animals

It was somewhat more difficult to identify the location of AI on the cortical surface in lesioned animals due to the disturbance of the sulcal pattern caused by the neonatal lesions (cf. Fig. 2). Large portions of the lateral gyrus were removed in some cases, causing the ectosylvian gyrus to be displaced posteromedially. However, we are reasonably confident that our injections were restricted to AI, based on cytoarchitectonic similarity of the region with AI in normal animals and also on the consistency of the location of retrograde label in both thalamus and cortex. For example, one extremely useful criterion was the presence of heavy label in the contralateral AI (Pallas et al., in prep.).

As in normal animals, retrograde label in the thalamus following injections of tracers into AI was quite heavy in the MGN, particularly in the ventral and medial divisions, and in parts of the posterior nucleus (PO) adjacent to the MGN. Label was also present in the dorsal division of MGN but was excluded from the caudal part of the dorsal division (Figs. 7, 8). Thus, this portion of the thalamocortical projection in lesioned animals does not appear to be different from normal.

A major difference between normal thalamocortical projections and those in lesioned animals concerned label in the dorsal portion of the thalamus. In the lesioned animals,

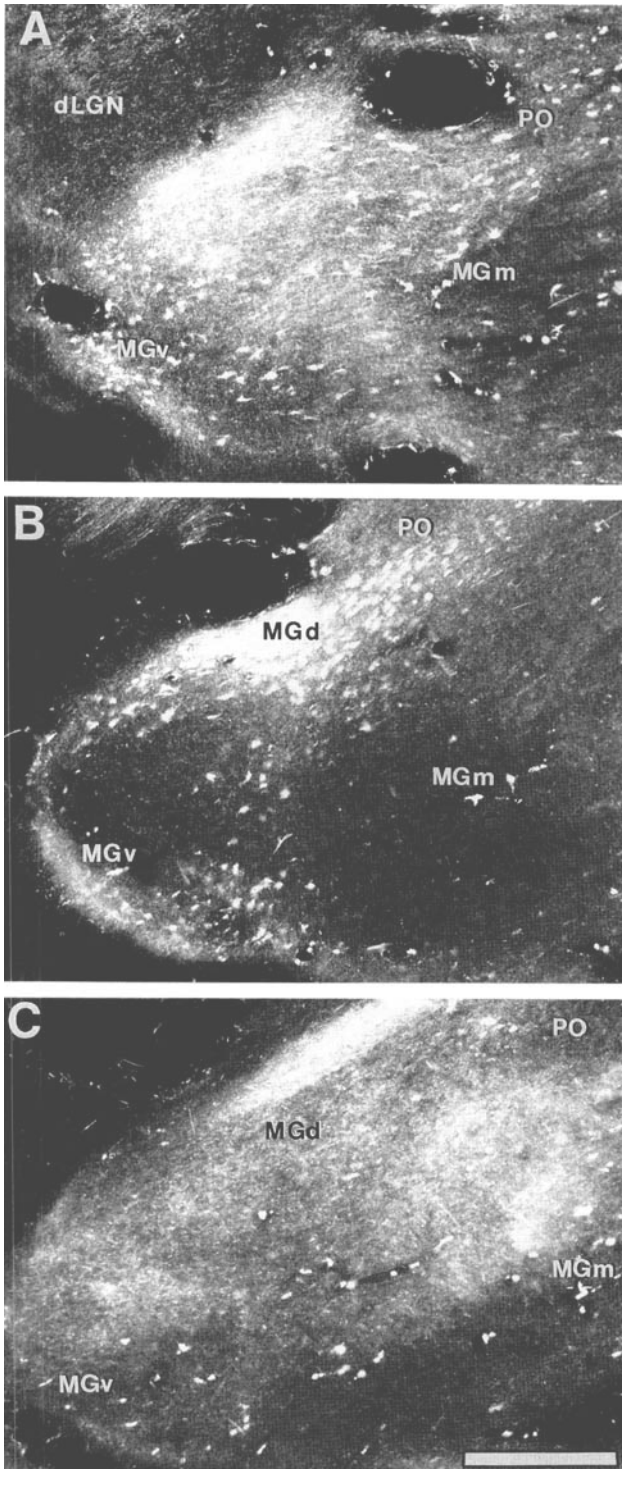

Fig. 4. Retrograde and anterograde label in MGN of a normal ferret following injection of HRP and WGA-HRP in AI. **A:** In this coronal section through the thalamus, the anterior portion of MGv is visible and contains anterograde and retrograde label. PO and MGm are labelled as well. **B:** This section is 1,000 μm posterior to the section shown in A. All major divisions of the MGN contain label, as does the PO. The dLGN and the LP/Pulvinar complex (not shown) do not contain any label. **C:** Another 500 μm posterior, anterograde and retrograde label can be seen in MGv, MGd, and MGm, as well as the PO group, but there are very few labelled somata in the MGv at this level. Scale bar: 200 μm.

we consistently saw retrogradely filled cells in the lateral posterior/pulvinar complex (LP/Pulvinar) following AI injections (Fig. 7, 8). In many cases (3 of 5), we also saw label in the lateromedial-suprageniculate (LM-Sg) thalamic area, which in the cat is normally connected reciprocally to the anterior ectosylvian visual area (Norita et al., '85) and the posterior ectosylvian gyrus (EPp, Bowman and Olson, '88), and which receives input from the deep layers of the superior colliculus (Graybiel and Berson, '80). This projection was completely absent in the normal animals (Figs. 4–6). We are confident that these anomalies were not a result of inaccurate placement of the injection; cytoarchitectonic criteria, the pattern of label in contralateral cortex (Pallas et al., in prep.) and MGN, and the pattern of label resulting from injections that were in fact placed outside of AI (see following paragraph) argue against this possibility.

The anomalous projection from the LP/Pulvinar complex to AI is also illustrated by injections in two other lesioned animals (Figs. 9 and 10). In each of these animals, there were heavy projections from the various divisions of the MGN to AI. The projections from the LP/Pulvinar were sparser in the animal shown in Figure 9 than in the one shown in Figure 10. In the latter case, however, the heaviest label in the LP/Pulvinar was due to an injection (FG label in Fig. 10) that was made slightly more medial than the medial edge of AI. In this animal, there were also some cells labelled in dLGN from the same injection. Label in the dLGN was not seen in any other case. While this particular animal had an extremely large cortical lesion, which removed all of the posterior lateral gyrus and part of the suprasylvian gyrus, examination of the injection site and the cortical cytoarchitecture shows that the injection site was located mainly in the lateral suprasylvian (LS) cortex, which receives input from the C-laminae of the dLGN in normal cats and which has been shown to receive direct inputs from the A-laminae following ablation of areas 17 and 18 in neonatal kittens (Kalil et al., '79; Tong et al., '84; see also Kavanagh and Kelly, '87). Consistent with the location of the Fluoro-Gold injection in LS cortex, the LS area in contralateral cortex contained retrogradely labelled cells (Pallas et al., in prep.), which were not seen in other ferrets with AI injections.

Thus, the major thalamic inputs to AI in the lesioned animals arose from the ventral, dorsal, and medial divisions of the MGN, from the posterior thalamic nucleus adjacent to the MGN, from the LM-Sg region, and from the LP/Pulvinar complex. The projections from LM-Sg and LP/Pulvinar are novel in the lesioned animals. Because of the possibility that the LP/Pulvinar projection could supply visual input to AI in lesioned animals independent of the retina-MGN-AI pathway, we undertook a series of eye injections to examine the extent of retinal terminals in the dorsal part of the thalamus.

Eye injections in normal and lesioned animals

Figure 11 shows the pattern of terminal label in the left thalamus following WGA-HRP injections into the right eye of a normal ferret. The label is very heavy in dLGN and the superior colliculus. In addition there is label present in the geniculate wing (GW, Guillery et al., '80) as well as some light label in the pretectal area. In contrast, eye injections in the lesioned animals contralateral to the lesioned hemisphere also produce patchy label in the MGN (cf. Fig. 11B; Sur et al., '88) and in the LP/Pulvinar complex (Figs. 11B, 12). These areas in the normal animals are completely devoid of label (cf. Fig. 11A). However, there appears to be

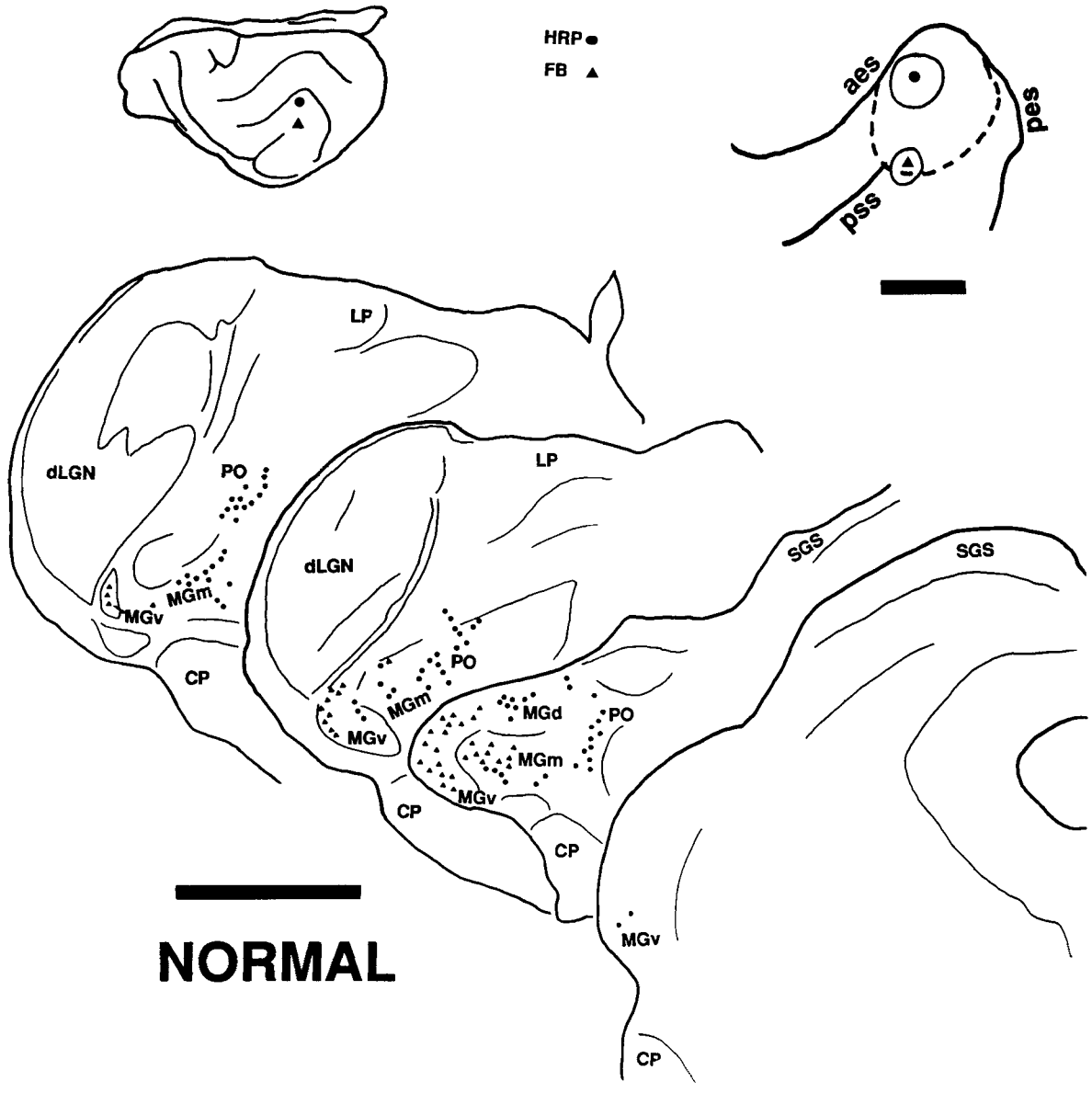

Fig. 5. A coronal reconstruction of the label resulting from tracer injections in AI (in a normal animal). The injection site (symbols) and surrounding halos of label (solid lines) in relation to AI (shown by dotted line) is shown on the top right. A view of the injection site in relation to the entire hemisphere is shown on the upper left. In the reconstruction, the pattern of label resulting from both the HRP and Fast Blue (FB) injections in AI is shown. Note that in all of the reconstructions, each symbol represents two or three labelled cells; we have not attempted to represent every labelled cell but rather have depicted relative density of retrograde label. Anterograde label was omitted from the reconstructions for clarity. Retrograde label is found in all three subdivisions of the MGN and in PO. Each injection site produced a slab of labelled cells extending rostrocaudally through the MGv. Note in the third section from the right that the more medial HRP injection labels a more medial slab of cells than the lateral injection of Fast Blue. Sections are 400 μm apart. Scale bar: 2 mm.

little overlap between the retinal terminal label in the LP/Pulvinar region and the somata that project from this region to AI (Figs. 8–10). Much of the heaviest retinal terminal label (arrows in Figs. 11, 12) is dorsal to the AI-projecting cells. The retinal terminal label in MGN, while not as dense as that in the LGN, overlaps extensively with the MGN somata backfilled from AI injections. We suggest from these data that the contribution of the LP/Pulvinar projection to visual response properties in AI is minimal compared with the projection from the MGN.

Topography of thalamocortical projections in normal and lesioned ferrets

Analysis of the topography and detailed pattern of connectivity between the thalamus and AI in normal and lesioned animals is complicated by several factors: comparisons have to be made across animals; the sizes of cortical and thalamic areas are distorted by the neonatal lesions; and injections of different tracers differ in effective spread, in uptake, and thus in their zones of retrograde thalamic label. Neverthe-

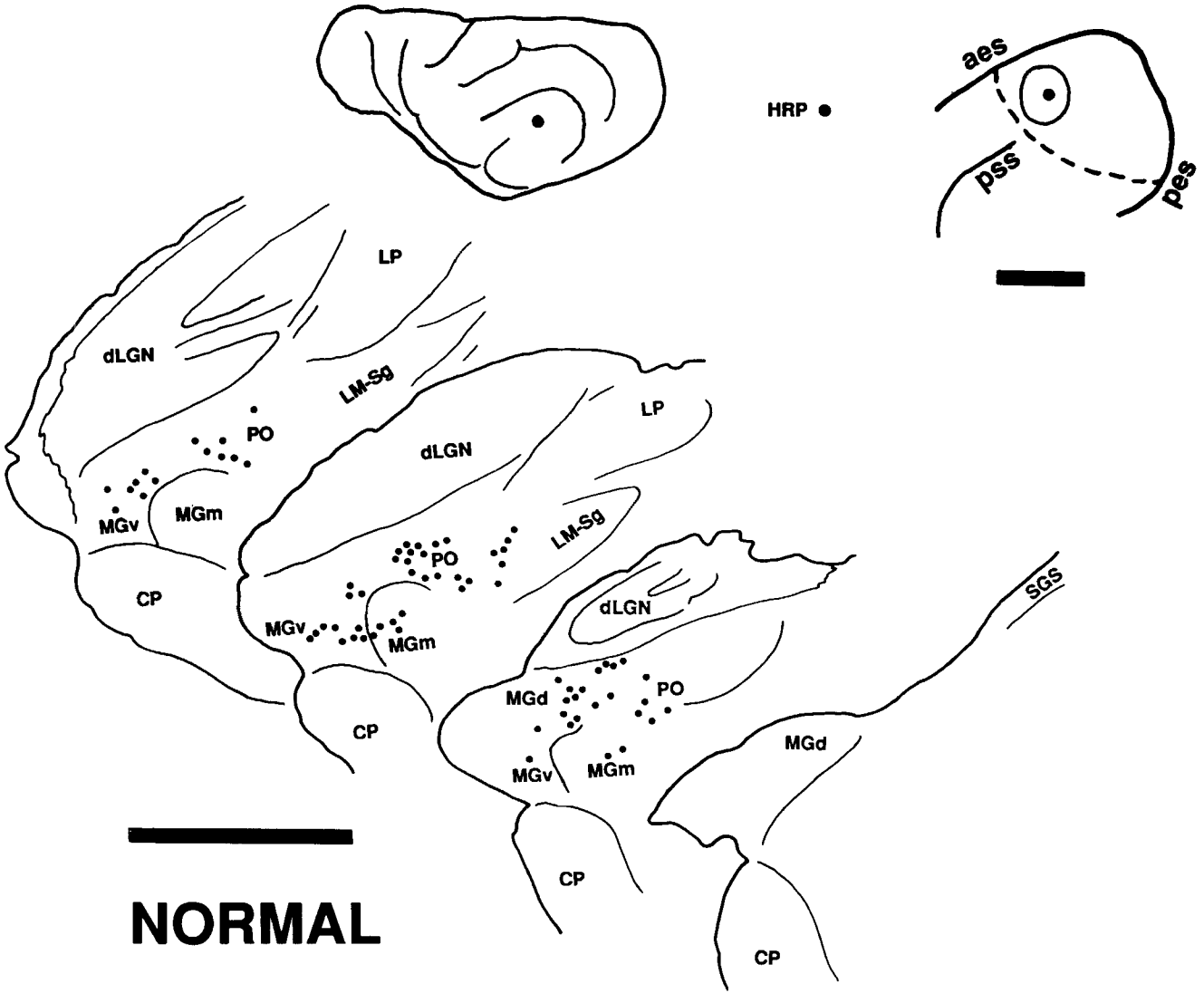

Fig. 6. A coronal reconstruction of the data from another normal animal. Conventions as in Figure 5. This shows another example of the pattern of retrograde thalamic label following HRP injection into AI. As in the other normals, label is seen throughout the MGN and PO, with the exception of the most caudal portion of MGN. Every two to three labelled cells is represented by a symbol. Sections are 500 μm apart. Scale bar: 2 mm.

less, several observations can be made that lead to some important generalizations and concepts regarding thalamocortical connectivity in the auditory pathway.

In normal animals, single injections in AI lead to retrogradely labelled cells in the ventral, dorsal, and medial divisions of the MGN, and in PO (Figs. 4, 5, 6). In MGv, which forms the principal thalamic nucleus projecting to AI, labelled cells are organized as curved bands that are often quite extensive in single coronal sections (e.g., the Fast Blue label in Fig. 5) and which can extend rostrocaudally through most of the nucleus. In this way, a slab of thalamic cells projects to a circumscribed locus in AI. In lesioned animals, single injections in AI lead to similar slabs of cells labelled in MGv (Figs. 8, 9). Thus, the thalamocortical projection from MGv to AI is similar in normal and lesioned animals (see below).

More detailed descriptions of the topography of thalamocortical projections between the MGN (particularly MGv) and AI in normal and lesioned ferrets require analysis of data from multiple tracer injections in AI. Multiple tracer injections in normal ferrets show that medial AI gets input from a slab of cells in medial MGv, and slabs of cells in lateral MGv project to lateral AI (Fig. 5). Because low sound frequencies are represented laterally and high frequencies medially within AI (Kelly et al., '86), the frequency representation in MGv must also increase from lateral to medial.

Injections of two different tracers at different sites in AI in lesioned animals can produce either an overlapped or nonoverlapped pattern of retrogradely labelled cells in MGv, depending on where the injection sites are located in AI. For example, in Figure 8, injection of two tracers retrogradely labels two different slabs of cells in MGv, and in Figure 9, the Fluoro-Gold and HRP injections label nonoverlapping slabs while the HRP and Rhodamine injections label a more overlapped set of cells. In some cases (F88-61 and F88-76; see Table 1), the detailed topography

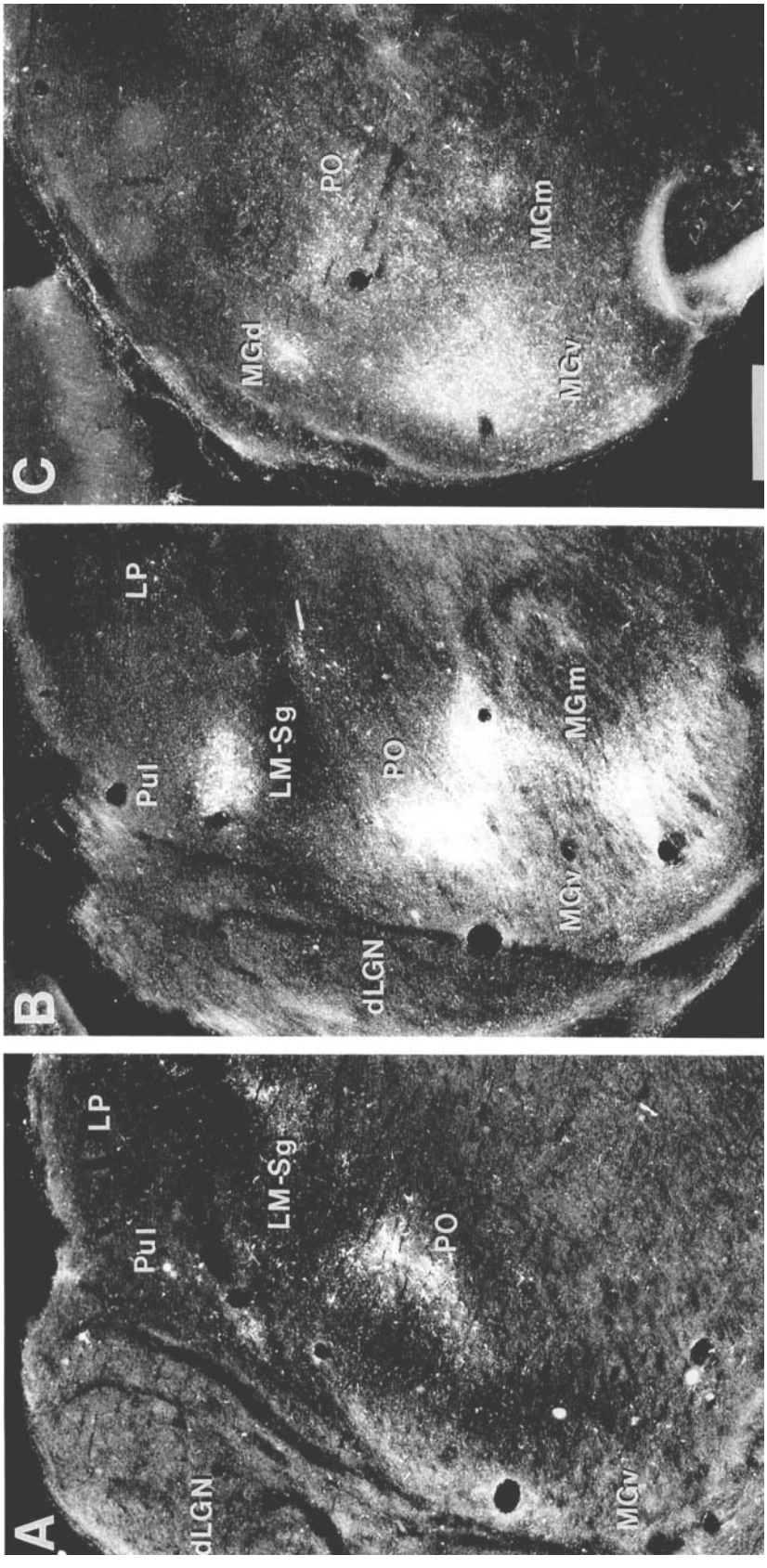

Fig. 7. A series of coronal sections showing the pattern of retrograde and anterograde HRP label in the thalamus of a ferret that received neonatal lesions rerouting retinal afferents to the MGN (see text). These sections are reconstructed in Figure 9. **A:** In this section, light label is present in the LM-Sg in addition to the heavier label in PO. The label in the dorsal part of the thalamus (including LP/Pul and LM-Sg) was never seen in normal animals. **B:** This section is 400 μm posterior to A. In addition to the MGN label, a heavy patch of label can be seen in dorsal thalamus on the border between the Pulvinar and the LM-Sg area. A few labelled cells can also be seen in LP on the right hand side of the micrograph. **C:** In this section through the MGN (500 μm posterior to B), label can be seen in all three subdivisions of the MGN and in PO. Scale bar: 0.5 mm.

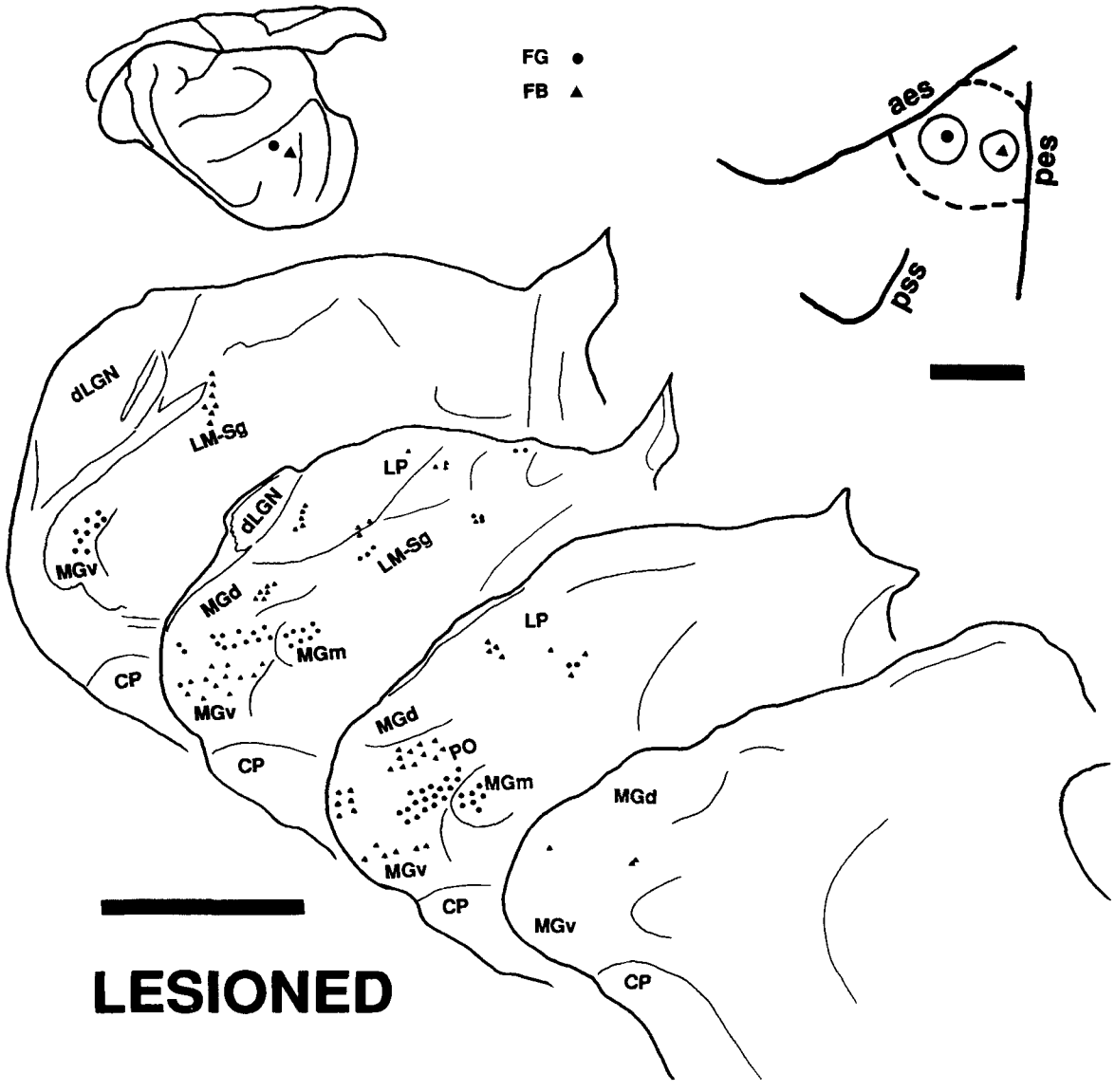

Fig. 8. Results from an injection of both Fluoro-Gold (FG) and Fast Blue (FB) in the ectosylvian gyrus (AI) of a ferret that received neonatal lesions directing retinal afferents into the MGN. These coronal sections in this reconstruction are 400 μm apart. The majority of the retrograde label is contained in the three subdivisions of the MGN and in PO. Discrete injections in AI lead to discrete slabs of label extending rostrocaudally in the MGN. Label is again found in the LP and LM-Sg nuclei in this lesioned animal. In normal animals label was never seen in these areas following injections into AI. Conventions as in Figure 5. Scale bar: 2 mm.

of the thalamocortical projection in the lesioned animals resembles that in normal ferrets; lateral MGv projects to more lateral AI and vice versa. In other cases (F88-24 and F88-34; see Table 1), it is difficult to determine if the normal pattern is retained. Because we have no physiological correlate of frequency representation in the lesioned animals (auditory input to the thalamus has been removed at birth), it is impossible to say whether injections of two different tracers lie in different frequency representations or within an isofrequency slab, and in general to what frequencies the injection sites correspond to. It is also true in ferrets (Kelly et al., '86), as it is in cats (Merzenich et al., '75, '82), that the orientation of the frequency map varies quite a bit between animals. However, within the limits of resolution of our techniques, we can tentatively conclude that the detailed pattern of projection between AI and MGv in both the variable and isofrequency axes is preserved in the lesioned animals, despite the absence of auditory input and the presence of anomalous visual inputs.

Topography within the projections to AI from other divisions of the thalamus is even harder to define at present. This is due in part to the sparse nature of these projections, especially in the case of the projections from LP/Pulvinar. In addition, the difficulty is compounded because the thalamic subnuclei have not yet been well described in the ferret.

Corticothalamic projections in lesioned animals

As in the normal animals, the pattern of corticothalamic projections in the lesioned animals reciprocated the thalamo-

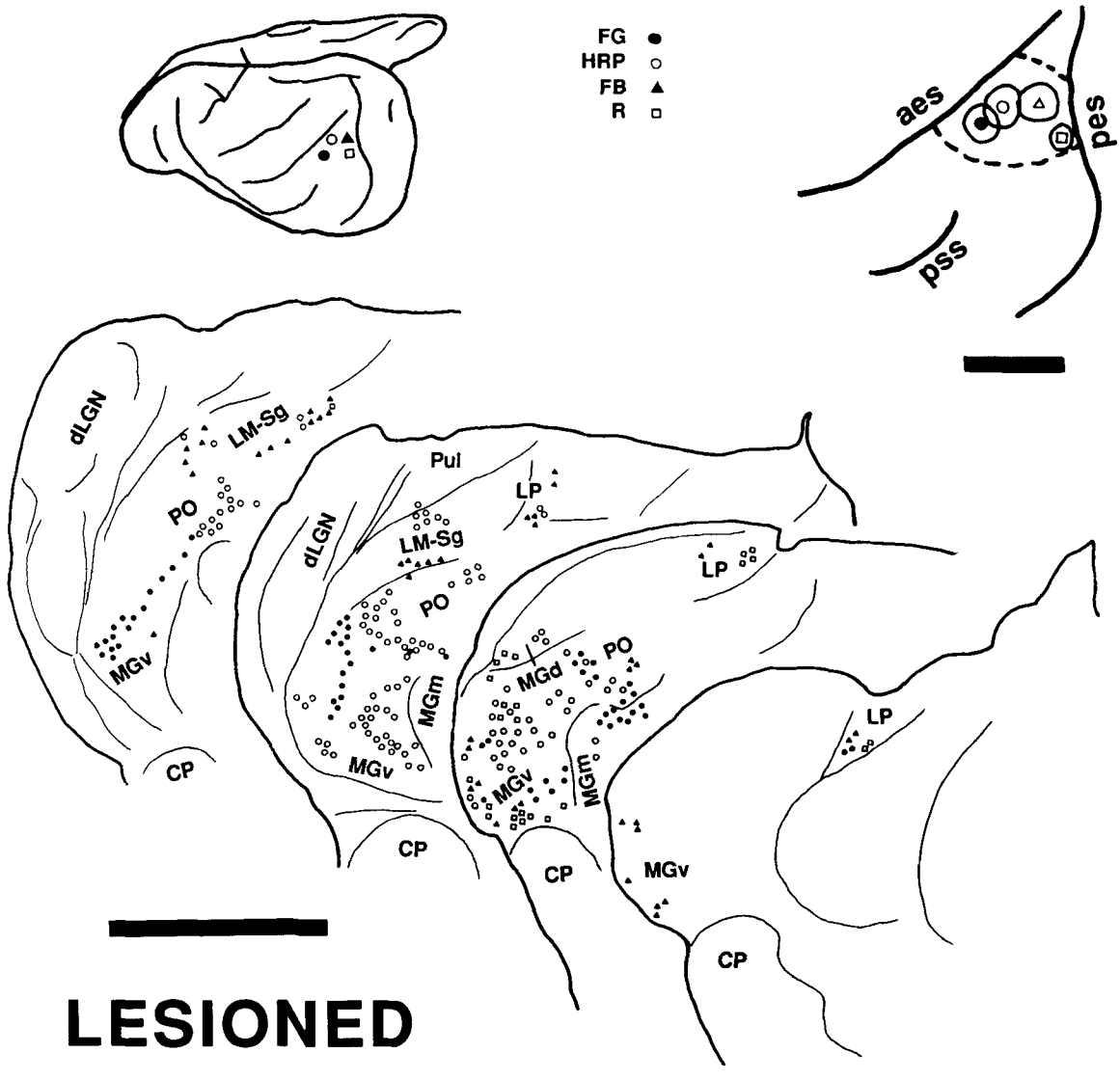

Fig. 9. A coronal reconstruction of the thalamus of the neonatally lesioned ferret shown in Figure 7 following injection of four different anatomical tracers in AI: Fluoro-Gold (FG), HRP mixed with WGA-HRP (HRP), Fast Blue (FB), and Rhodamine (R). Note the label in both the LP/Pul complex and the LM-Sg area which is not seen in normal animals. The injection of four tracers at different points allows determination of the topography of the thalamocortical projection. See text for details. Sections are 400 μm apart. Conventions as in Figure 5. Scale bar: 2 mm.

cortical projection very closely. This reciprocal pattern included the LP/Pulvinar area, though the anterograde label in the MGN/PO area was much heavier than that in LP/Pulvinar.

DISCUSSION

There are two major results of this study. First, in ferrets with visual projections routed into the auditory pathway, we find that thalamic projections to AI arise mainly from the MGN and PO as in normal ferrets. In addition, there are sparser, novel projections to AI from the LP/Pulvinar region in the lesioned ferrets. Second, the topography of projections to AI from MGv, the major division of the MGN, resembles the MGv-AI projections in normal ferrets. In the following, we will first discuss the similarities in thalamocortical projections in the auditory pathway between normal ferrets and cats (which have been studied more extensively to date) and then discuss the two major results from the lesioned animals.

Comparison of thalamocortical connections in the auditory pathway of normal ferrets and cats

As stated earlier, our identifications of thalamic nuclei in ferrets are based on similarities in location and cytoarchitecture with thalamic nuclei in cats. We have confined our delineations of the dorsal part of the thalamus and the auditory thalamus to their major subdivisions: LP, Pulvinar, and LM-Sg in the dorsal part of the thalamus, and MGv, MGd and MGm in the auditory thalamus, and we

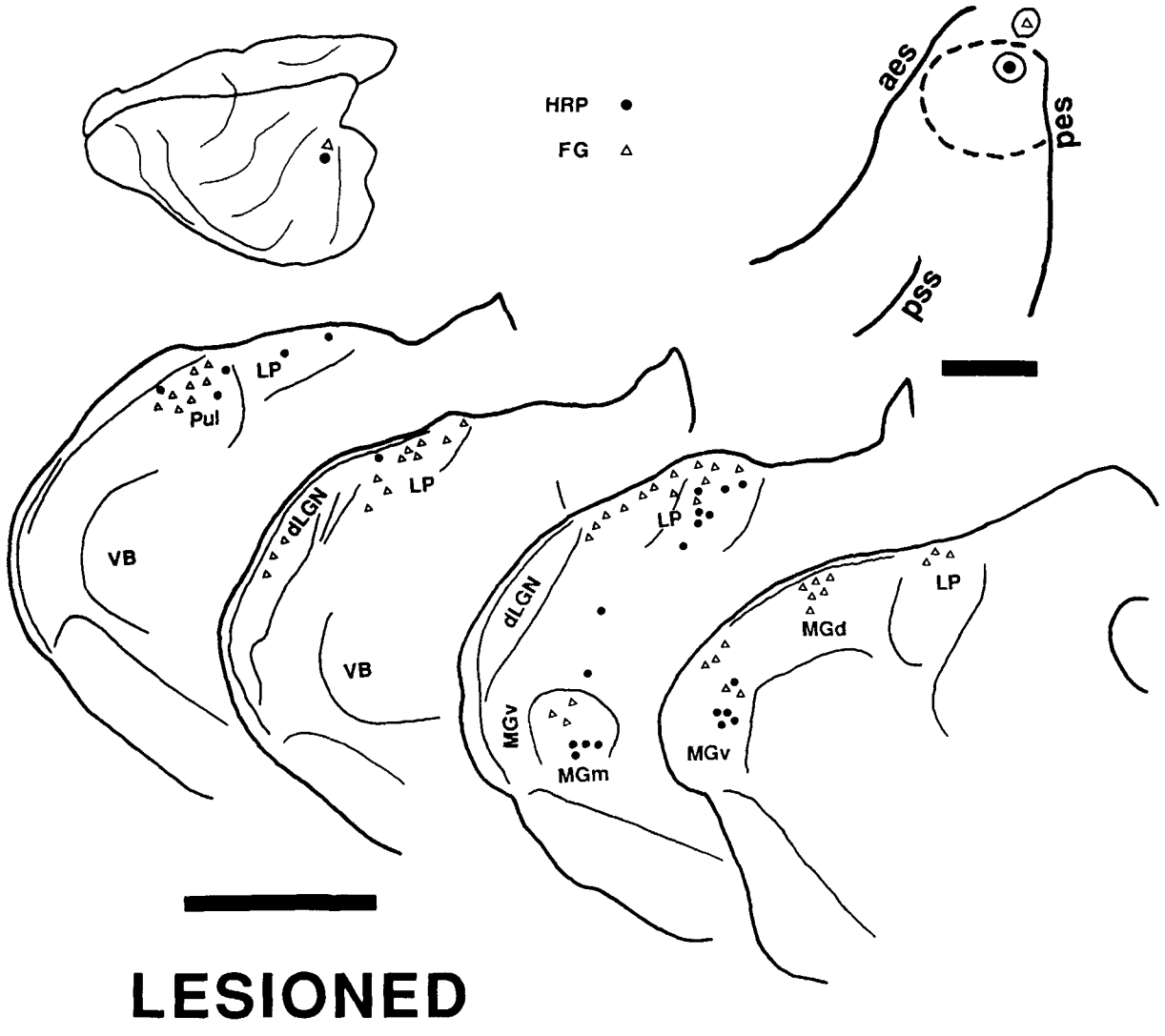

Fig. 10. Coronal reconstruction of thalamic retrograde label in a lesioned ferret following injections of HRP in AI and Fluoro-Gold (FG) in the lateral suprasylvian visual cortical area. The label in the dorsal thalamus was quite heavy in this animal and the Fluoro-Gold label extended into the dLGN. Sections are 400 μm apart. Conventions as in Figure 5. Scale bar: 2 mm.

make no attempt to subdivide these nuclei further. While we are confident of our categorization, more detailed identification must await physiological, connectional, and Golgi studies of the ferret thalamus.

Although it was not the purpose of this study to describe in detail the anatomy of the normal ferret auditory system, our control animals do provide substantial information in this regard. Our results suggest that the normal patterns of auditory thalamocortical and corticothalamic connectivity in the ferret are quite similar to what has been described in the cat. This is perhaps not unexpected, as both the ferret and cat are in the Family Carnivora. Thalamic input to AI arises from the dorsal, ventral, and medial divisions of MGN and from PO. As in the cat, the ventral division of the MGN projects densely to AI, which in turn projects back to the thalamus in a reciprocal way. The projection from PO to AI is also quite heavy. Some authors in fact consider the PO to be part of the MGN (e.g., Andersen et al., '80), which from our results would seem appropriate.

Because we have not obtained best frequency data from our injection sites, we cannot determine the tonotopic organization of the ferret MGN. However, Kelly et al. ('86) have mapped the ferret AI, showing that high frequencies are represented medially and low frequencies laterally. Our results suggest that lateral AI receives input from lateral MGN and medial AI from medial MGN, suggesting the frequency representation in the normal ferret MGv increases from lateral to medial. In the cat MGv, frequency representation also increases from lateral to medial (Andersen et al., '80), despite the fact that the tonotopic map in the cat AI is rotated 90 degrees with respect to that in the ferret (i.e., isofrequency lines in the cat AI run dorsoventrally, but run anteroposteriorly in the ferret (Merzenich et al., '75; Reale and Imig, '80; Kelly et al., '86; Phillips et al., '88). A thorough mapping study may reveal more subtle differences between the thalamic frequency maps in cat and ferret.

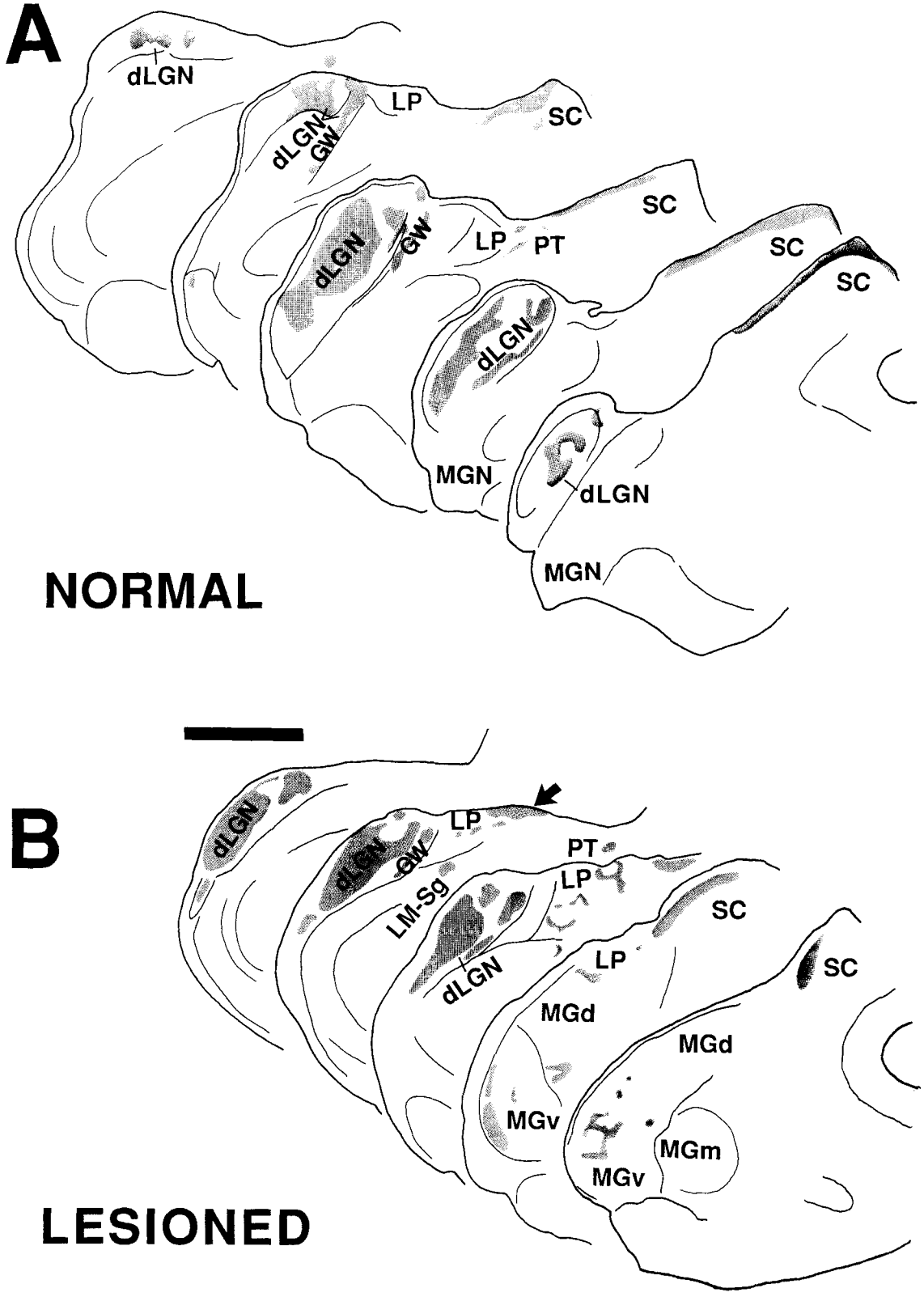

Fig. 11. The pattern of terminal label following injections of a mixture of HRP and WGA-HRP in the right eye of a normal (**A**) and lesioned (**B**) ferret. In addition to the normal target areas in A, lesioned animals have retinal terminals in the MGN and LP. The LP label is sparse compared to the MGN label, however, and is mostly dorsal (arrow) to the location of cell bodies whose axons project to AI. Coronal sections are 400 μm apart. Scale bar: 2 mm.

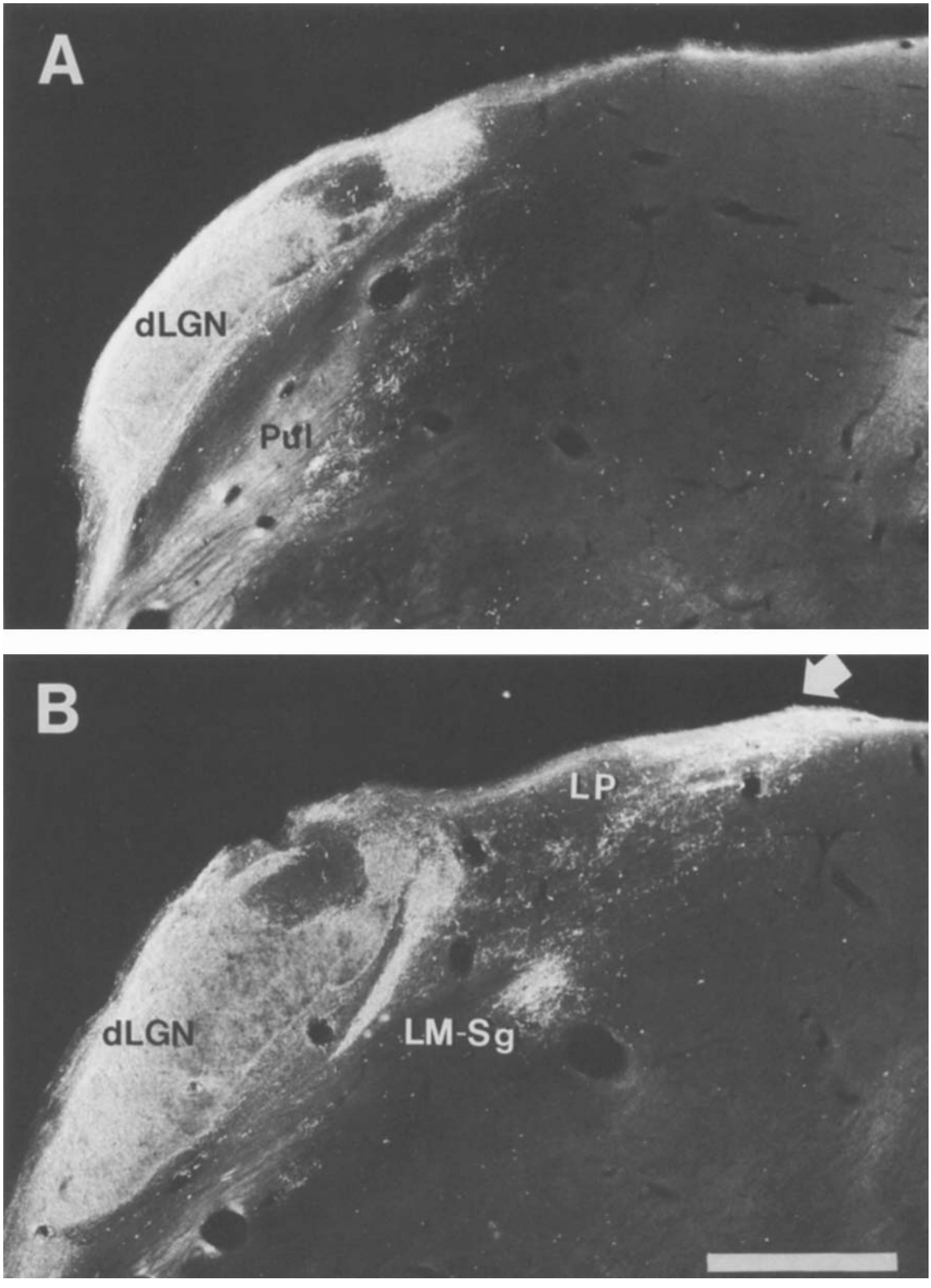

Fig. 12. Micrographs from the neonatally lesioned animal used to make the reconstruction in Figure 11B. In addition to heavy retinal terminal label in the dLGN, sparse label is seen in the LP/Pul complex and in LM-Sg. The section in B is 500 μm posterior to the section in A. The arrow in B points out the dorsal LP label indicated by the arrow in Figure 11. Scale bar: 0.5 mm.

Potential visual inputs to AI

One purpose of this study was to establish whether or not there are visual projections from the retina through the thalamus into AI in the lesioned ferrets from sources other than the MGN. We have indeed demonstrated that there are anomalous inputs to AI from the dorsal part of the thalamus. Most of this novel projection arises from the LP nucleus, but there are also inputs to AI from the pulvinar and the LM-Sg area. We have also demonstrated anomalous retinal input to LP/Pulvinar. Other evidence suggests, however, that visual input does not reach AI from cortical areas receiving direct or indirect visual input through the surviving fragment of dLGN (Pallas et al., '88), so that the dorsal portion of the thalamus is apparently the only potential source of visual information to AI other than the MGN.

While we cannot rule out the possibility that visual input can reach AI from the retina via the LP/Pulvinar complex, it seems unlikely that this projection could play a major role in the response properties of visual cells in AI. First, the LP/Pulvinar-AI projection is quite sparse as compared to the MGN/PO-AI projection. Second, most of the retinal input to the LP/Pulvinar complex lies dorsal to the cells which project to AI. In contrast, retinal projections to MGN overlap considerably with MGN cells that project to AI. Though the projection from the retina to the MGN is not very extensive, the highly divergent projections from MGv to AI suggest that large regions of AI can be influenced by restricted portions of MGv (see also below).

Novel retinal projections to the MGN and to LP/Pulvinar

Neither the MGN nor the LP/Pulvinar complex normally receive direct retinal input [with the exception of the geniculate wing, which has been defined by some authors as a part of the dLGN (Guillery et al., '80) and by others as the retinal recipient zone of the pulvinar (Leventhal et al., '80)]. The LP nucleus acquires its visual function via inputs from the SC, pretectum and cortical areas 17, 18, 19, and LS (Updyke, '76, '77, '79; Graybiel and Berson, '80), while the pulvinar receives input from the pretectum (Graybiel and Berson, '80). However, as we have shown, both the MGN and the LP/Pulvinar complex receive direct visual input in the lesioned ferrets (Figs. 11B, 12). These projections are due to sprouting and not due to retention of transient collaterals of retinofugal fibers (Linden et al., '81; Hahm and Sur, '88).

The early lesions of SC and visual cortex made in the lesioned ferrets, which reduce retinal targets in the thalamus and midbrain, also deprive the LP nucleus of a substantial portion of its inputs (LP receives input from SC and visual cortex; Graybiel and Berson, '80). This deafferentation may be responsible for the sprouting of retinal afferents into the area (Schneider, '73). Rabbits with early ablations of primary visual cortex have expanded retinal projections to LP (Murphy et al., '88). Also, in cats that have had early ablations of areas 17, 18, and 19, thereby partially deafferenting LP, anomalous retinal projections to LP occur, along with increased retinal projections to the GW (Labar et al., '81; Kalil, personal communication). In the case of the MGN as well, deafferentation is necessary for novel retinal inputs to enter the nucleus (Sur et al., '88; Roe et al., in prep.).

We do not know what class of retinal ganglion cells project to the LP/Pulvinar complex in the lesioned animals. In normal cats, retinal projections to the neighboring geniculate wing (Guillery et al., '80) appear to arise from a subpopulation of W-cells (Leventhal et al., '85). We have provided anatomical and physiological evidence that W-cell axons grow into the MGN in our lesioned ferrets (Sur et al., '88), and we have also suggested that more than one subpopulation of W-cell axons may be capable of such plasticity (Roe et al., '87; Pallas et al., '89).

Novel projections from the LP/Pulvinar complex to AI

These projections may result from retention of exuberant projections that are normally eliminated with development, or from sprouting of new projections. There is currently no evidence for transient LP-AI projections in the cat, but the issue has not been thoroughly examined yet in kittens, and we cannot distinguish between the two possibilities at this time. In either case, LP probably projects to AI because part of its normal cortical target areas have been ablated.

Regarding the possibility that the projections arise from exuberant collaterals, it is relatively unusual for thalamocortical projections to show plasticity of this type. They do not exhibit the exuberance that is seen in the projections of cortical cells but rather form targeted projections that are topographically specific (Rakic, '76; Crandall and Caviness, '84). This early specificity may explain why minimal reorganization is seen following damage to the thalamocortical system. For example, rather than forming extensive new connections, the lateral geniculate nucleus largely degenerates following removal of its cortical target areas in several species (Perry and Cowey, '79; Pearson et al., '81; Raabe et al., '86; see also Miller et al., '87).

The minimal plasticity that is seen in thalamocortical projections usually occurs within functional systems (Kaas et al., '83; Kalil, '84; Kalil et al., '79). Cross-modal plasticity in thalamocortical projections has not been demonstrated previously. In one respect, however, we cannot consider the projections from LP to primary auditory cortex in our lesioned animals to be cross-modal; we have induced visual activity in AI via retinal projections to MGN. If the visual activity itself is what allows the LP-AI projection to occur, then we must consider the hypothesis that the modality of the inputs to a target structure can influence its other inputs and outputs.

Projections from the MGN to AI in lesioned animals

The second goal of this study was to examine the detailed nature of projections from the MGN to AI in lesioned animals, in order to assess whether retinal inputs to the MGN alter its characteristic thalamocortical connectivity patterns. Studies in Siamese cats show that the pattern of projections from the dLGN to striate cortex can change in response to variations in retinogeniculate projections. Furthermore, the geniculocortical projection might compensate in different ways (Hubel and Wiesel, '71; Kaas and Guillery, '73; Cooper and Blasdel, '80) for the additional crossed pathway from temporal retina to the dLGN that is characteristic of Siamese cats (Guillery and Kaas, '71).

Conversely, thalamocortical connections can retain relatively normal precision and order despite drastic alterations in their input. Removal of both eyes very early in development in ferrets (Guillery et al., '85), tree shrews (Brunso-

Bechtold and Casagrande, '81), and monkeys (Rakic, '88), before most dLGN cells are generated or before geniculocortical afferents enter the cortical plate, causes massive atrophy and shrinkage of the dLGN and shrinkage of the surface area of striate cortex. However, the remaining geniculocortical connections develop topographically and remain so, despite the absence of visual input. Similarly, congenitally anopthalmic mice retain relatively normal geniculocortical projections (Kaiserman-Abramof et al., '80).

We were able to compare the projections from MGN to AI in normal and lesioned animals in some detail and have found substantial similarities. Specifically, a focal injection in AI of both normal and lesioned ferrets produces retrograde label in a slab of MGN cells through the MGv (Fig. 13A). The anterograde label from HRP injections also follows this pattern. The anterior to posterior axis of AI in normal ferrets is an axis of isofrequency representation; cells along this axis all respond to the same sound frequency (Kelly et al., '86). Isofrequency laminae have also been identified in the MGv of the cat (Imig and Morel, '85; Morel and Imig, '87).

We have no direct evidence in normal ferrets on how isofrequency laminae in MGv interconnect with isofrequency slabs in AI. The evidence in cats, however, suggests a highly divergent and convergent projection between isofrequency slabs or laminae in MGv and in AI. That is, single tracer injections in AI retrogradely label nearly all of an isofrequency lamina in MGv, and injections of multiple tracers along the isofrequency axis in AI lead to highly overlapped populations of labelled cells in MGv (Merzenich et al., '82, '84). More recent evidence in cats suggests some topographic order within the isofrequency dimension in the projections from MGN to AI (Brandner and Redies, '90). However, in all studies of thalamocortical connections in the auditory pathway of cats to date, particularly those in which single injections of retrograde tracers were made in AI, the spread of labelled cells in the isofrequency dimension of the MGN is significantly greater than the spread of labelled cells in the tonotopic dimension (Andersen et al., '80; Middlebrooks and Zook, '83; Morel and Imig, '87; Brandner and Redies, '90). In the high-frequency representations within MGv and AI, the isofrequency slabs are subdivided into binaural groups (EE and EI cells, Middlebrooks and Zook, '83), and the slab-to-slab projections between MGv and AI are specific for binaural type, keeping EE and EI cells segregated from each other. Thus, slabs of cells labelled in MGv from single discrete injections into AI in our normal ferrets would correspond to isofrequency laminae in MGv.

In lesioned animals, the fact that slabs of cells are labelled in MGv following single AI injections suggests that "isofrequency laminae" persist in MGv in the absence of auditory input (Fig. 13B). In lesioned ferrets, of course, "isofrequency laminae" are simply anatomical constructs, since auditory inputs to the thalamus have been removed at birth.

The slab-to-slab connections that exist between the MGv and AI might imply extensive convergence and divergence of single thalamic axon arbors in AI, or simply neighboring cells in the MGN projecting to disparate loci in AI. There are at least two physiological implications of this anatomical finding, particularly if the major route for visual inputs to AI is from the retina through MGv, as we suggest. First, even though retinal input to the MGN in general, and to MGv in particular, occupies only a fraction of the entire

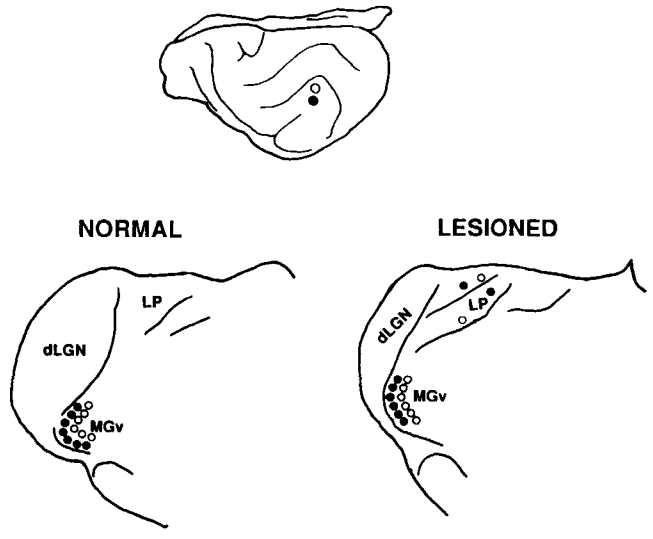

Fig. 13. Summary of results. Injections of retrograde tracers in AI of normal ferrets produce slabs of label in MGv extending rostrocaudally through the nucleus. The topography of the MGv to AI projection in lesioned animals resembles that in normal ferrets. Our results suggest that medial MGv projects to medial AI (open circles), while lateral MGv projects to lateral AI (closed circles). Label is also found in the other two main divisions of the MGN and in PO (not shown in diagram). In the lesioned animals, in addition to the label in MGN and PO, label is found in the dorsal thalamus, including LP, Pul, and LM-Sg.

volume of the MGN (retinal terminals in MGN occur in clumps with much of the nucleus devoid of retinal terminals; Figs. 11, 12; see also Sur et al., '88), a much larger portion of AI can potentially receive visual input. Indeed, we find that while most recording sites in AI of lesioned animals are visually responsive (Sur et al., '88; Roe et al., '88), many recording sites in the MGN are not (our unpublished observations).

The second implication of slab-to-slab projections from MGv to AI in lesioned ferrets is that, from the anatomical projections alone, one would not expect spatially restricted receptive fields or a systematic two-dimensional visual field map in AI. This can be readily appreciated by contrasting the nature of thalamocortical projections in the auditory pathway between MGv and AI with those in the visual pathway between dLGN and striate cortex. In the latter case, the projections from the retina, through the plane of each layer of the dLGN, to the plane of layer 4 in striate cortex, can be schematized as point-to-point, with relatively limited convergence and divergence and a relatively focal representation in cortex of each point on the retina. In contrast, the slab-to-slab projection between MGv and AI suggests that, in general, each neuron or cluster of neurons in an "isofrequency" slab will represent the same extensive strip of retina. Adjacent "isofrequency" slabs would represent adjacent retinal strips.

However, we find that visually responsive neurons in AI have spatially localized receptive fields, and that there is a systematic two-dimensional representation of visual space in AI (Roe et al., '88). We suggest that this might occur by an anatomical selectivity at the synaptic level, or by physiological sharpening within AI, so that single neurons in AI express, in topographically ordered fashion, only a subset of the visual inputs they receive. The underlying mechanism

could involve lateral inhibitory connections and an activity-dependent sharpening mechanism based on correlated activity between neighboring locations in the retina, similar to the sharpening that occurs in the retinotectal projection in fish and frogs (see Constantine-Paton, '82; Schmidt and Edwards, '83; Schmidt and Eisele, '85). At least along the isofrequency dimension, this mechanism could employ the same lateral inhibitory circuitry that sharpens frequency selectivity in the normal AI.

CONCLUSIONS

Our early lesions (which remove the visual cortex and the major targets of the retina and deafferent the MGN) are associated with anomalous projections from the dorsal part of the thalamus to AI. At this point, we cannot determine whether these novel projections are a result of an active redirection of thalamic axons into AI as a result of its newly acquired visual quality, or whether thalamic axons from the dorsal part of the thalamus will simply sprout into any neighboring territory when their normal target is lost. However, the connections between auditory thalamus and primary auditory cortex appear to be unaffected by the change in modality of the information carried by the thalamocortical afferents. The detailed organization of the MGv to AI projection in the cat is controversial at present (see Brandner and Redies, '90). If substantial topographic order is shown to exist along the isofrequency dimension in the projections from MGv to AI, it would follow that such projections themselves could lead to a retinotopic map in AI. At this time, however, we interpret the connections between MGv and AI as highly convergent and divergent, and we suggest that the retinotopic map formed within AI in our lesioned ferrets results from processing intrinsic to the cortex itself.

ACKNOWLEDGMENTS

This work was supported by NIH postdoctoral grant EY 06121 to S.L.P. and NIH grant EY 07719, a March of Dimes grant, and a McKnight Foundation grant to M.S. We are grateful to Dr. Barbara L. Finlay and Dr. Paul S. Katz for their insightful comments on an earlier version of this manuscript. We also thank Teresa Sullivan for excellent technical assistance and Jong-on Hahm and Henry Hall for their expert assistance with photomicrography.

LITERATURE CITED

Andersen, R.A., P.L. Knight, and M.M. Merzenich (1980) The thalamocortical and corticothalamic connections of AI, AII, and the anterior auditory field (AAF) in the cat: Evidence for two largely segregated systems of connections. J. Comp. Neurol. *194:*663–701.

Berman, A.L., and E.G. Jones (1982) The Thalamus and Basal Telencephalon of the Cat. Madison, WI: University of Wisconsin Press.

Bowman, E.M., and C.R. Olson (1988) Visual and association areas of the cat's posterior ectosylvian gyrus: Thalamic afferents. J. Comp. Neurol. *272:*15–29.

Brandner, S., and H. Redies (1990) The projection from medial geniculate to Field AI in cat: Organization in the isofrequency dimension. J. Neurosci. *10:*50–61.

Brunso-Bechtold, J.K., and V.A. Casagrande (1981) Effect of bilateral enucleation on the development of layers in the dorsal lateral geniculate nucleus. Neuroscience *6:*2579–2586.

Constantine-Paton, M. (1982) The retinotectal hookup: The process of neural mapping. In S. Subtelny and P.B. Green (eds): Developmental Order: Its Origin and Regulation. New York: Alan R. Liss, pp. 317–349.

Cooper, M.L., and G.C. Blasdel (1980) Regional variation in the representation of the visual field in the visual cortex of the Siamese cat. J. Comp. Neurol. *193:*237–253.

Crandall, J.E., and V.S. Caviness (1984) Thalamocortical connections in newborn mice. J. Comp. Neurol. *228:*542–556.

Frost, D.O. (1981) Ordered anomalous retinal projections to the medial geniculate, ventrobasal and lateral posterior nuclei. J. Comp. Neurol. *203:*227–256.

Frost, D.O. (1986) Development of anomalous retinal projections to nonvisual thalamic nuclei in Syrian hamsters: A quantitative study. J. Comp. Neurol. *252:*95–105.

Geneser-Jensen, F.A., and T.W. Blackstad (1971) Distribution of acetylcholinesterase in the hippocampal region of the guinea pig. I. Entorhinal area, parasubiculum, and presubiculum. Z. Zellforsch. Mikrosk. Anat. *114:*460–481.

Graybiel, A.M., and D.M. Berson (1980) Histochemical identification and afferent connections of subdivisions in the lateralis posterior-pulvinar complex and related thalamic nuclei in the cat. Neuroscience *5:*1175–1238.

Guillery, R.W., E.E. Geisert, Jr., E.H. Polley, and C.A. Mason (1980) An analysis of the retinal afferents to the cat's medial interlaminar nucleus and to its rostral thalamic extension, the "geniculate wing." J. Comp. Neurol. *194:*117–142.

Guillery, R.W., and J.H. Kaas (1971) A study of normal and congenitally abnormal retinogeniculate projections in cats. J. Comp. Neurol. *143:*73–100.

Guillery, R.W., M. Ombrellaro, and A.L. LaMantia (1985) The organization of the lateral geniculate nucleus and of the geniculocortical pathway that develops without retinal afferents. Devel. Brain Res. *20:*221–233.

Hahm, J.-O., and M. Sur (1988) The development of individual retinogeniculate axons during laminar and sublaminar segregation in the ferret LGN. Soc. Neurosci. Abstr. *14:*460.

Hubel, D.H., and T.N. Wiesel (1971) Aberrant visual projections in the Siamese cat. J. Physiol. *218:*33–62.

Imig, T.J., and A. Morel (1985) Tonotopic organization in ventral nucleus of medial geniculate body in the cat. J. Neurophysiol. *53:*309–340.

Kaas, J.H., and R.W. Guillery (1973) The transfer of abnormal visual field representations from the dorsal lateral geniculate nucleus to the visual cortex in Siamese cats. Brain Res. *59:*61–95.

Kaas, J.H., M.M. Merzenich, and H.P. Killackey (1983) The reorganization of somatosensory cortex following peripheral nerve damage in adult and developing mammals. Ann. Rev. Neurosci. *6:*325–356.

Kaiserman-Abramof, I.R., A.M. Graybiel, and W.J.H. Nauta (1980) The thalamic projection to cortical area 17 in a congenitally anopthalmic mouse strain. Neuroscience *5:*41–52.

Kalil, R.E. (1984) Removal of visual cortex in the cat: Effects on the morphological development of the retino-geniculo-cortical pathway. In J. Stone, B. Dreher, and D.H. Rapaport (eds): Development of the Visual Pathways in Mammals. New York: Alan R. Liss, Inc., pp. 257–274.

Kalil, R.E., L. Tong, and P.D. Spear (1979) Reorganization of geniculocortical pathways in the cat following neonatal damage to the visual cortex. Invest. Opthal. Vis. Sci. Suppl. *18:*157.

Karnovsky, M.J., and L. Roots (1964) A "direct-coloring" thiocholine method for cholinesterases. J. Histochem. Cytochem. *12:*219–221.

Kavanagh, G.L., and J.B. Kelly (1987) Contribution of auditory cortex to sound localization by the ferret (*Mustela putorius*). J. Neurophysiol. *57:*1746–1766.

Kelly, J.B., P.W. Judge, and D.P. Phillips (1986) Representation of the cochlea in primary auditory cortex of the ferret (*Mustela putorius*). Hearing Res. *24:*111–115.

Labar, D.R., N.E. Berman, and E.H. Murphy (1981) Short- and long-term effects of neonatal and adult visual cortical lesions on the retinal projection to the pulvinar in cats. J. Comp. Neurol. *197:*639–659.

Leventhal, A.G., J. Keens, and I. Tork (1980) The afferent ganglion cells and cortical projections of the retinal recipient zone (RRZ) of the cat's "pulvinar complex." J. Comp. Neurol. *194:*535–554.

Leventhal, A.G., B. Dreher, and R.W. Rodieck (1985) Central projections of cat retinal ganglion cells. J. Comp. Neurol. *237:*216–226.

Linden, D.C., R.W. Guillery, and J. Cucchiaro (1981) The dorsal lateral geniculate nucleus of the normal ferret and its postnatal development. J. Comp. Neurol. *203:*189–211.

Merzenich, M.M., S.A. Colwell, and R.A. Andersen (1982) Auditory forebrain organization: Thalamocortical and corticothalamic connections in the cat. In C.N. Woolsey (ed): Cortical Sensory Organization. Clifton, NJ: Humana Press, pp. 43–57.

Merzenich, M.M., W.M. Jenkins, and J.C. Middlebrooks (1984) Observations and hypotheses on special organizational features of the central auditory nervous system. In G.M. Edelman, W.E. Gall, and W.M. Cowan (eds): Dynamic Aspects of Neocortical Function. New York, NY: Neurosciences Research Foundation, pp. 397–424.

Merzenich, M.M., P.L. Knight, and G.L. Roth (1975) Representation of cochlea within primary auditory cortex in the cat. J. Neurophysiol. *38:*231–249.

Mesulam, M.M. (1978) Tetramethyl benzidine for horseradish peroxidase histochemistry: A non-carcinogenic blue reaction product with superior sensitivity for visualizing neural afferents and efferents. J. Histochem. Cytochem. *26:*106–117.

Middlebrooks, J.C., and J.M. Zook (1983) Intrinsic organization of the cat's medial geniculate body identified by projections to binaural response-specific bands in the primary auditory cortex. J. Neurosci. *3:*203–224.

Miller, B., M.S. Windrem, L. Anllo-Vento, and B.L. Finlay (1987) Minor reorganization of thalamocortical projections following large neonatal thalamic lesion in the golden hamster. Soc. Neurosci. Abstr. *13:*1419.

Morel, A., and T.J. Imig (1987) Thalamic projections to fields A, AI, P, and VP in the cat auditory cortex. J. Comp. Neurol. *265:*119–144.

Morest, D.K. (1964) The neuronal architecture of the medial geniculate body of the cat. J. Anat. *98:*611–630.

Morest, D.K. (1965) The laminar structure of the medial geniculate body of the cat. J. Anat. *99:*143–160.

Murphy, E.H., A.M. Grigonis, T.E. Hayden, D. Tashayyod, and M. Wilkes (1988) The effects of ablation of visual cortex in neonatal rabbits on the organization of retinothalamic and retinopretectal projections. Devel. Brain Res. *38:*27–35.

Norita, M., L. Mucke, G. Benedeck, B. Albowitz, Y. Katoh, and O.D. Creutzfeldt (1985) Connections of the anterior ectosylvian visual area (AEV). Exp. Brain Res. *174:*1–16.

Otsuka, R., and R. Hässler (1962) Uber Aufbau und Gliederung der corticalen Sehsphäre bei der Katze. Arch. Psychiat. Nervenkrankh. *203:*212–234.

Pallas, S.L., A.W. Roe, and M. Sur (1988) Retinal projections induced into auditory thalamus in ferrets: Changes in inputs and outputs of primary auditory cortex. Soc. Neurosci. Abstr. *14:*460.

Pallas, S.L., J.-O. Hahm, and M. Sur (1989) Retinal axon arbors in a novel target: Morphology of ganglion cell axons induced to arborize in the medial geniculate nucleus of ferrets. Soc. Neurosci. Abstr. *15:*495.

Pearson, H.E., D.R. Labar, B.R. Payne, P. Cornwaell, and N. Aggarwal (1981) Transneuronal retrograde degeneration in the cat following neonatal ablation of visual cortex. Brain Res. *212:*470–475.

Perry, V.H., and A. Cowey (1979) The effects of unilateral cortical and tectal lesions on retinal ganglion cells in rats. Exp. Brain Res. *35:*97–108.

Phillips, D.P., P.W. Judge, and J.B. Kelly (1988) Primary auditory cortex in the ferret (*Mustela putorius*): Neural response properties and topographic organization. Brain Res. *443:*281–294.

Raabe, J.I., M.S. Windrem, and B.L. Finlay (1986) Control of cell number in the developing visual system. II. Visual cortex ablation. Dev. Brain Res. *28:*1–11.

Rakic, P. (1976) Prenatal genesis of connections subserving ocular dominance in the rhesus monkey. Nature *261:*467–471.

Rakic, P. (1988) Specification of cerebral cortical areas. Science *241:*170–176.

Reale, R.A., and T.J. Imig (1980) Tonotopic organization in auditory cortex of the cat. J. Comp. Neurol. *192:*265–291.

Roe, A.W., P.E. Garraghty, and M. Sur (1987) Retinotectal W-cell plasticity: Experimentally induced retinal projections to auditory thalamus in ferrets. Soc. Neurosci. Abstr. *13:*1023.

Roe, A.W., S.L. Pallas, J. Hahm, Y.H. Kwon, and M. Sur (1988) Retinal projections induced into auditory thalamus in ferrets: Visual topography in primary auditory cortex. Soc. Neurosci. Abstr. *14:*460.

Rose, J.E. (1949) The cellular structure of the auditory region of the cat. J. Comp. Neurol. *91:*408–440.

Sanides, F., and J. Hoffmann (1969) Cyto- and myeloarchitecture of the visual cortex of the cat and of the surrounding integration cortices. J. Hirnforsch. *11:*79–104.

Schmidt, J.T., and D.L. Edwards (1983) Activity sharpens the map during the regeneration of the retinotectal projection in goldfish. Brain Res. *269:*29–39.

Schmidt, J.T., and L.E. Eisele (1985) Stroboscopic illumination and dark rearing block the sharpening of the regenerated retinotectal map in goldfish. Neurosci. *14:*535–546.

Schneider, G. (1973) Early lesions of the superior colliculus: Factors affecting the formation of abnormal retinal projections. Brain Behav. Evol. *8:*73–109.

Sur, M., P.E. Garraghty, and A.W. Roe (1988) Experimentally induced visual projections into auditory thalamus and cortex. Science *242:*1437–1441.

Sur, M., S.L. Pallas, and A.W. Roe (1990) Cross-modal plasticity in cortical development: differentiation and specification of sensory neocortex. Trends Neurosci. *13:*227–233.

Tong, L., R.E. Kalil, and P.D. Spear (1984) Critical periods for functional and anatomical compensation in lateral suprasylvian visual area following removal of visual cortex in cats. J. Neurophysiol. *52:*941–960.

Updyke, B.V. (1976) Retinotopic organization in the pulvinar and lateral posterior complex of the cat. Anat. Rec. *184:*552.

Updyke, B.V. (1977) Topographic organization of the projections from cortical areas 17, 18, and 19 onto the thalamus, pretectum, and superior colliculus in the cat. J. Comp. Neurol. *173:*81–122.

Updyke, B.V. (1979) Projections from lateral suprasylvian cortex to the lateral posterior complex in the cat. Anat. Rec. *193:*707–708.